



**HAL**  
open science

## Experimental investigation of the early-age mechanical behaviour of oil-well cement paste

Nicolaine Agofack, Siavash Ghabezloo, Jean Sulem, André Garnier,  
Christophe Urbanczyk

### ► To cite this version:

Nicolaine Agofack, Siavash Ghabezloo, Jean Sulem, André Garnier, Christophe Urbanczyk. Experimental investigation of the early-age mechanical behaviour of oil-well cement paste. *Cement and Concrete Research*, 2019, 117, pp.91 - 102. 10.1016/j.cemconres.2019.01.001 . hal-03486654

**HAL Id: hal-03486654**

**<https://hal.science/hal-03486654>**

Submitted on 20 Dec 2021

**HAL** is a multi-disciplinary open access archive for the deposit and dissemination of scientific research documents, whether they are published or not. The documents may come from teaching and research institutions in France or abroad, or from public or private research centers.

L'archive ouverte pluridisciplinaire **HAL**, est destinée au dépôt et à la diffusion de documents scientifiques de niveau recherche, publiés ou non, émanant des établissements d'enseignement et de recherche français ou étrangers, des laboratoires publics ou privés.



Distributed under a Creative Commons Attribution - NonCommercial 4.0 International License

# Experimental investigation of the early-age mechanical behaviour of oil-well cement paste

Nicolaine Agofack<sup>a,b,c</sup>, Siavash Ghabezloo<sup>a,1</sup>, Jean Sulem<sup>a</sup>, André Garnier<sup>b</sup>, Christophe Urbanczyk<sup>b</sup>

<sup>a</sup> Laboratoire Navier, Ecole des Ponts ParisTech, Ifsttar, CNRS UMR 8205, Marne la Vallée, France

<sup>b</sup> TOTAL, Exploration & Production, CSTJF Pau, France

<sup>c</sup> Currently at SINTEF-Petroleum & NTNU, Trondheim, Norway

## ABSTRACT

The knowledge of the behaviour of oil-well cement paste from the early age to the hardened state is important in predicting the performances of the cement sheath in oil/gas wells, specially for prediction of the risk of micro-annulus creation between the cement sheath and the rock formation or the casing. Characterization of the early-age mechanical behaviour is of particular importance, because during the well construction, the cement sheath is submitted to various mechanical loadings when the cement paste is not completely hydrated, as for example during a casing test. In this paper, the early-age mechanical behaviour of a class G cement paste is studied experimentally. A specially designed experimental device is used to investigate the mechanical behaviour of cement paste from the first hour of hydration, under stress states close to in-situ conditions. The macroscopic shrinkage of the cement paste as well as its stress-strain response under oedometric loading are studied for various pressures during hydration, from 0.3 to 45 MPa, and for hydration temperatures from 7 to 30°C. These relatively low temperatures are used to slow down the hydration rate. The experimental results show that the macroscopic shrinkage increases significantly with the pressure during hydration. When submitted to a mechanical loading cycles at a given age, the cement paste hydrated under lower pressures, corresponding to shallower depth, exhibits higher deformability, showing a higher risk of creation of a micro-annulus during the mechanical loadings, as for example during a casing test. The experimental results clearly show the influence of the loading history on the mechanical behaviour of the cement paste at a given age. The oedometric experiments are associated with UCA (Ultrasonic Cement Analyser) and isothermal calorimetry experiments for a deeper insight into the behaviour of early age cement paste.

**Keywords:** early-age, cement hydration, shrinkage, stress–strain response, cement sheath, residual strain.

---

<sup>1</sup> Corresponding author: Siavash Ghabezloo, Laboratoire Navier, Ecole des Ponts ParisTech, 6&8 av. Blaise Pascal, Cité Descartes, 77455, Marne-la-Vallée cedex 2, France, Email : siavash.ghabezloo@enpc.fr

32        **1. Introduction**

33        In oil and gas industry, when drilling exploration or development wells, a mud is used to support the  
34        walls of the geological formation, to maintain the wellbore stability, to cool and clean the drill bit, to  
35        carry out the cuttings and to provide hydrostatic pressure which helps in preventing formation fluids to  
36        enter into the wellbore. Steel tubular (called "*casing*") is then run into the well and a cement slurry is  
37        pumped to fill the annulus space between two casings or between the casing and the geological  
38        formation. The cement slurry hardens progressively and forms a cement sheath, which plays an  
39        important role for well integrity. Along the well, it provides zonal isolation of different fluids (i.e.  
40        separation of different fluids, water, gas and oil); it protects the tubular against corrosion and provides  
41        mechanical support. The loss of cement-sheath integrity can result in the pressurization of the annulus,  
42        in gas migration up to a shallower formation or to the surface, and, in catastrophic cases, in a blowout  
43        and significant damage of the infrastructure.

44        The cement paste is an evolving porous material, its state changes progressively from fluid to solid  
45        during the hydration process. Along a well, different compositions of cement slurries can be used and  
46        their hydration takes place in different conditions of temperature and pressure depending on depth.  
47        Therefore, at a given time, cement paste behaviour and properties depend on the slurry composition of  
48        the cement paste including water-to-cement mass ratio (w/c), presence of additive agents, hydration  
49        conditions in terms of temperature and pressure. In addition, during the life of a well, from drilling to  
50        completion, production and P&A (plug and abandonment), the cement sheath is submitted to various  
51        mechanical and thermal loadings that can potentially damage its principal properties and alter its  
52        performance. According to some authors [1, 2] the increase of pressure during drilling can exceed 40  
53        MPa in the oil wells, and the applied pressure during a casing test can vary from a few tens of MPa in  
54        normally pressurized reservoirs to more than 80 MPa in high pressure reservoirs. These loadings may  
55        result in non-reversible deformation of cement sheath and consequently the creation of a micro-  
56        annulus in the cement-casing or cement-rock interface. This is particularly important when these  
57        loadings are applied at relatively early age, when the mechanical properties and strength of the cement  
58        paste are not yet completely developed. As it was reported in the literature [3, 4, 5], at the early-age,  
59        the shrinkage of cement paste and the decrease of its pore pressure are considered to be the main  
60        causes of leakage in oil and gas wells. However, very few experimental data exist on the mechanical  
61        properties (macroscopic shrinkage, elastic modulus, the stress-strain behavior) of the hydrating oil-  
62        cement in field conditions and at very early age. Some properties, particularly the macroscopic  
63        shrinkage, have been extensively studied for civil engineering applications in which the cement paste  
64        is hydrated under ambient pressure and temperature conditions. The situation is quite different for oil-  
65        well applications in which the cement paste is hydrated under various conditions of pressure and  
66        temperature, depending mainly on the depth and reservoir conditions.

67 This work is dedicated to an experimental study of the mechanical behavior of early-age cement paste,  
68 during the first 6 days of hydration under various pressures and temperatures. A specially designed  
69 experimental device is used to investigate the macroscopic shrinkage of cement paste and its stress-  
70 strain response under oedometric conditions, from the first hour of hydration. To investigate the effect  
71 of early-age loading history on long-term properties, classical triaxial experiments are performed on  
72 hardened samples submitted to various loadings at their early age. The tested material is a class G oil-  
73 well cement, with water-to-cement ratio equal to 0.44. The same material has been continuously  
74 studied by the co-authors providing a rich database of mechanical, hydraulic, thermal and  
75 microstructure properties [6, 7, 8, 9, 10, 11, 12, 13, 14] [15]. The hydration conditions correspond to a  
76 temperature range from 7 to 30°C and a pressure range from 0.3 to 45 MPa. These relatively low  
77 temperatures are used to slow down the cement hydration kinetics. These experiments are associated  
78 with UCA (Ultrasonic Cement Analyser) and isothermal calorimetry experiments for a deeper insight  
79 into the behaviour of early age cement paste.

## 80 **2. Experimental devices and tests procedures**

81 To study the mechanical behavior of the cement paste at very early-age, one should be able to apply  
82 mechanical loadings on the hydrating paste without modifying its hydration conditions of temperature  
83 and pressure. This is a difficult task in a classical testing procedure in which the sample's temperature  
84 and pressure are generally brought back to ambient conditions before installing it in the loading cell.  
85 The hydration progress during this procedure and the dependence of the cement paste microstructure  
86 on temperature during hydration make it difficult to control the conditions at which the experiment is  
87 performed. To overcome these difficulties, a special uniaxial strain (oedometric) cell was designed by  
88 TOTAL in which the cement paste is poured immediately after mixing, and hydrated under controlled  
89 conditions of temperature and pressure. The cement paste can be submitted to mechanical loading  
90 cycles, at any time even before setting, without modifying its hydration conditions, what is impossible  
91 in a standard triaxial cell.

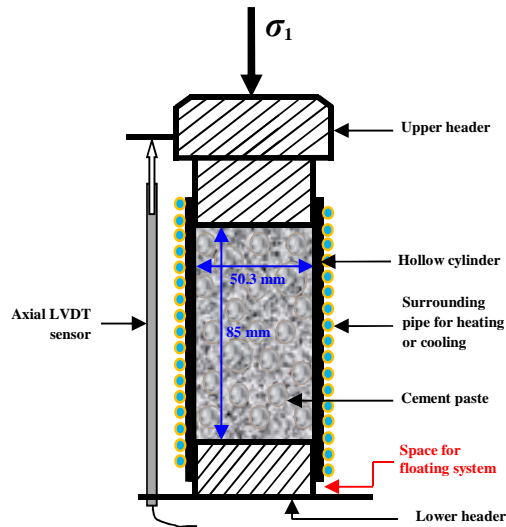


**Figure 1. Uniaxial-strain (oedometric) equipment**

92 The oedometric cell, shown in Figure 1, is composed of a hollow cylinder (50.3 mm of internal  
 93 diameter, 90 mm of external diameter and 125 mm height) made of steel. Within its elastic domain,  
 94 the hollow cylinder can support a maximum pressure of 123 MPa applied on its inner surface. The  
 95 hollow cylinder is surrounded by a cooling/heating system, connected to a cryostat, whereby cold/hot  
 96 fluid is circulated through a small-diameter tubing. The axial displacement of the sample is measured  
 97 by a Linear Variable Differential Transformer (LVDT). An electromechanical ram, able to apply 650  
 98 kN, is used to apply the axial stress. The oedometric cell is cooled or heated to the test temperature  
 99 before the preparation of the slurry.

100 **The tested specimen has a diameter of 50.3 mm and a height of 85mm.** The axial displacement of the  
 101 cement paste is measured continuously during hydration. At a given age, a mechanical loading cycle is  
 102 applied to the hydrating paste to measure its oedometric (P-wave) modulus and to study its stress-  
 103 strain response. In order to compare this “static” oedometric modulus with the dynamic (P-wave  
 104 modulus), experiments are performed in similar hydration conditions using an Ultrasonic Cement  
 105 Analyzer (UCA) apparatus which permits to continuously measure the P-wave velocity (at ultrasonic  
 106 frequency) on the hydrating cement paste. In oedometric cell, as well as in UCA apparatus, the  
 107 properties of the hydrating cement paste are measured as function of time. In order to analyze the  
 108 experimental results as a function of the degree of hydration, a high pressure high temperature (HPHT)  
 109 calorimeter is used to evaluate the hydration kinetics from the measurement of hydration heat. A  
 110 standard triaxial cell is also used to analyse the effect of loading history at very early-age on the long-  
 111 term properties.

112 **To analyze the pore size distribution, the mercury intrusion porosimetry (MIP) is performed on**  
 113 **samples with different histories of hydration. The sample dimensions are 25 mm in diameter and 20**  
 114 **mm in height. After drying the samples by freeze-drying, the mercury is injected into the sample under**

115 controlled pressure. At each pressure level the quantity of injected mercury enables calculating the  
116 porosity and the applied pressure is used to estimate the corresponding pore entry size.

117 All tests were performed on a slurry made of CEMOIL class G cement (API classification), the  
118 chemical composition of which is presented in Table 1. The cement slurry is composed of class G  
119 cement powder, distilled and deaerated water with  $w/c = 0.44$ , and three additive agents (anti-foaming,  
120 dispersing and anti-settling), as presented in Table 2.

121 **Table 1. Chemical Composition of a class G cement (Blaine = 323 m<sup>2</sup>/kg)**

Chemical composition	Measures	API recommendations Spec 10A
Magnesium oxide (MgO) %	1.8	Max 6.0
Sulfurtrioxide (SO <sub>3</sub> ) %	2.5	Max 3.0
Loss on ignition %	0.6	Max 3.0
Insoluble residue %	0.10	Max 0.75
C <sub>3</sub> A %	2.1	Max 3.0
C <sub>4</sub> AF + 2 C <sub>3</sub> A %	17.4	Max 24.0
C <sub>3</sub> S %	58.9	Min 48.0/ Max 65.0
(0.658 × K <sub>2</sub> O) + Na <sub>2</sub> O %	0.55	Max 0.75

122

123 **Table 2. Composition of 600 ml of cement slurry:  $w/c = 0.44$ , density = 1900 ± 10 kg/m<sup>3</sup>)**

Components	Quantity (grams)
Cement (class G)	783.53
water (distilled and deaerated)	339.54
Anti-foaming (D047)*	6.27
Dispersing agent (D604AM)*	9.47
Anti-settling (D153)*	1.18

124

\* commercial identification of the product

125

126 Distilled and deaerated water is poured into the mixing container, which is then placed on the mixer  
127 base. The dry anti-settling agent is added to the water and the motor is turned on and maintained to  
128 4000 ± 200 rotations per minutes for 5 minutes of agitation. Then the liquid anti-foaming and  
129 dispersing agents (poured before cement) and the cement powder are put successively into the  
130 container in 20 ± 5 seconds, (according to API [16], cement powder shall be added in 15s). The speed  
131 is immediately increased to about 12 000 ± 500 rotations per minute and mixing ended automatically  
132 after 35 ± 1 seconds.

133

### 3. Reliability and repeatability of the oedometric tests

134

In order to test the reliability of the oedometric test, distilled water is put into the cell. The mechanical loading path of Figure 2a consists of an increase of the axial stress from 5 to 25 MPa, followed by a decrease from 25 to 5 MPa. After maintaining the axial stress at 5 MPa for about 5 minutes, the same loading is again applied. This experiment is equivalent to an isotropic compression on water. The slope of axial stress – axial strain curve gives the bulk modulus of water. The result, presented in Figure 2b, gives the bulk modulus of water equal to 2.09 GPa which is very close to the value found in the literature. Thus, we conclude that the oedometric cell gives reliable results.

135

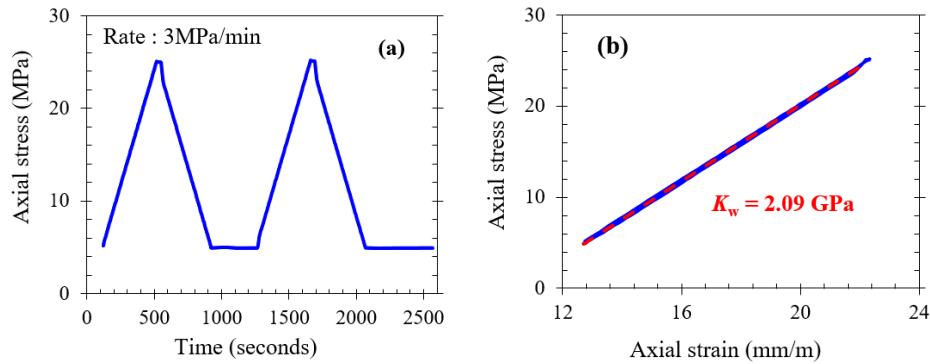
136

137

138

139

140



141

Figure 2. Reliability test: (a) loading path, (b) stress-strain behaviour and bulk modulus.

142

143

The repeatability of the oedometric tests is examined by performing three different tests with similar cement slurry and under the same conditions of hydration in terms of temperature and axial stress. The cement slurry is put into the oedometric cell previously cooled down at 7°C and the axial stress is then increased immediately to 25 MPa and kept constant. The evolution of the axial strain is measured as a function of time (or hydration). The result is displayed in Figure 3 and shows an excellent repeatability. In conclusion, the oedometric cell gives reliable and repeatable results. The nomenclature of the tests adopted in this study is *T* followed by the temperature during hydration and *P* followed by the axial stress or pressure during hydration. For example, T7P25 corresponds to the sample hydrated at a temperature of 7°C and under an axial stress of 25 MPa.

144

145

146

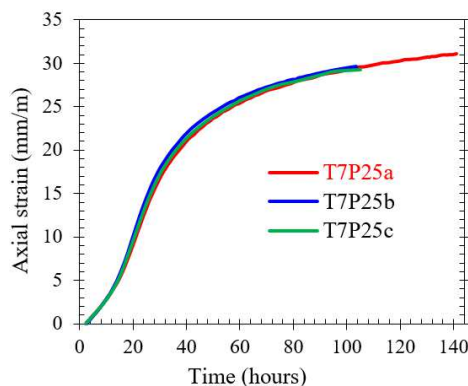
147

148

149

150

151



152

153 **Figure 3. Repeatability of the oedometric tests: three cement sample hydrated at 7°C and under 25 MPa**  
154 **of axial stress.**  
155

#### 156 **4. Experimental results and discussion**

157 During the cement hydration, the sum of the volumes of consumed cement clinker and water is higher  
158 than the volume of the produced hydrates. The difference represents the *chemical shrinkage* [17, 18].  
159 The chemical shrinkage results in pore pressure decrease within the cement paste during hydration. As  
160 a consequence, the effective stress increases and leads to a decrease of the external macroscopic  
161 volume of the hydrating cement paste. When the cement paste is hydrated at constant ambient  
162 temperature and under atmospheric pressure, this external volume decrease is called *autogenous*  
163 *shrinkage* [19, 18]. A different term, *macroscopic shrinkage*, is generally used when the hydration and  
164 the resulting volume change take place under pressure higher than the atmospheric pressure and/or  
165 temperature different to ambient temperature [18, 20, 17]. The macroscopic shrinkage of cement paste  
166 was measured in several studies [18, 20, 21] and more recently by Abuhaikal et al. [22]. In this  
167 section, we present a method to measure the macroscopic shrinkage of the cement paste and its stress-  
168 strain behaviour without modifying the condition of hydration. The effect of temperature and pressure  
169 of hydration on macroscopic shrinkage are analysed. The effect of age and macroscopic shrinkage on  
170 stress-strain behaviour of cement paste are also analysed.

#### 171 **4.1. Hydration kinetics**

172 The experiments presented in this paper are performed on cement pastes hydrated in a temperature  
173 range within 7°C and 22°C, under stresses between 0.3 and 45 MPa. It is known that the hydration  
174 kinetics is generally accelerated by increasing **the temperature and pressure during** hydration [23, 24,  
175 25, 26]. The knowledge of the hydration kinetics of the cement paste in the performed oedometric  
176 experiments is important for a better understanding and interpretation of the results. A high pressure  
177 high temperature calorimeter is used to evaluate the hydration kinetics from the measurement of  
178 hydration heat. **Calorimeter data provide the cumulative heat of hydration  $Q(t)$  released until a given**  
179 **time  $t$ . The degree of hydration can be evaluated through the following equation:**

$$180 \quad \xi(t) = \frac{Q(t)}{Q_{T\_CP}} \quad (1)$$

181 **where  $Q_{T\_CP}$  is the total cumulative heat released at complete hydration, which can be estimated by**  
182 **knowing the composition of the cement paste, using the following relation.**

$$183 \quad Q_{T\_CP} = \sum_X m_{X\_CP} Q_T^X \quad (2)$$



184 were  $m_{X,CP}$  represents the mass fraction of the compound X in the cement paste. The Table 3 gives  
 185 the details of calculation of  $Q_{T,CP}$ , assuming the main compounds of cement paste to be: water, alite,  
 186 belite, aluminate and ferrite. Detailed calculation of the volume fractions of the constituents for the  
 187 tested cement can be found in [27, 28].

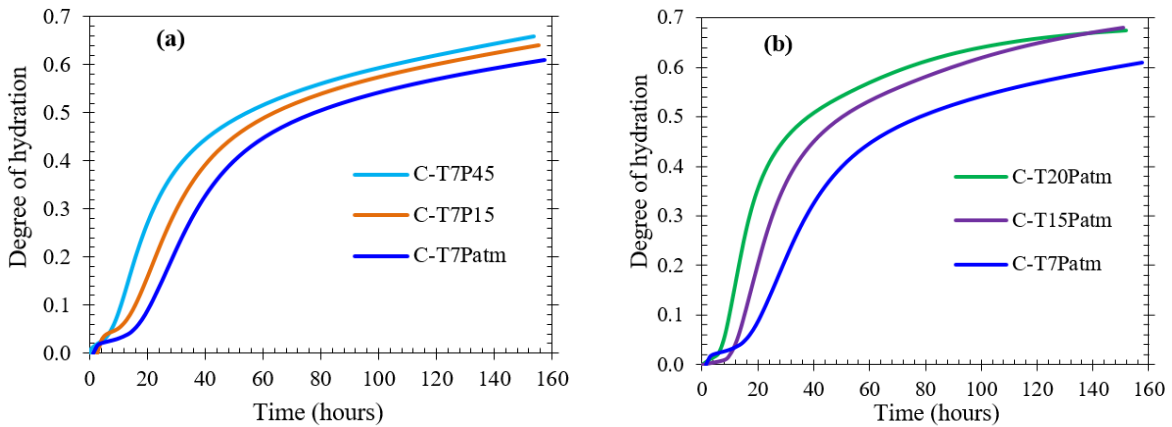
188  
 189

**Table 3. Estimation of hydration heat of a class G cement paste (w/c = 0.44)**

Compounds	Chemical composition	$Q_T^X$ (J/g)	$m_{X,CP}$	$Q_{T,CP}$ (J/g)
Water	H <sub>2</sub> O	0	0.3	297
Alite	C <sub>3</sub> S	500	0.427	
Belite	C <sub>2</sub> S	260	0.106	
Aluminate	C <sub>3</sub> A	900	0.010	
Ferrite	C <sub>4</sub> AF	420	0.111	

190

191 The results are presented in Figure 4 as function of time for different conditions of hydration. For a  
 192 given temperature during hydration (Figure 4a), the degree of hydration increases with the increase of  
 193 pressure. The same effect is observed for different temperatures when the pressure during hydration is  
 194 kept constant (Figure 4b).



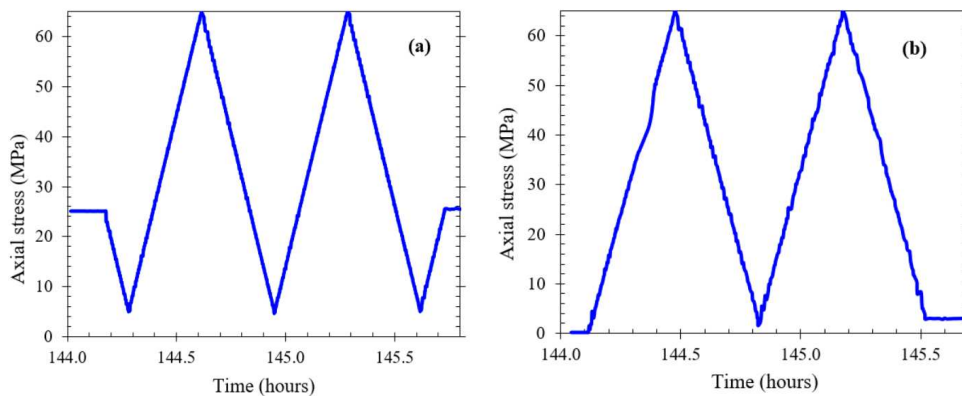
195  
 196  
 197

**Figure 4. Degree of hydration as function of time for different conditions of hydration in term of temperature and pressure.**

198 The presented results are compatible with the well-known pressure and temperature dependency of  
 199 cement hydration kinetics [24, 29, 30, 25, 31, 27].

200 **4.2. Typical results of an oedometric test**

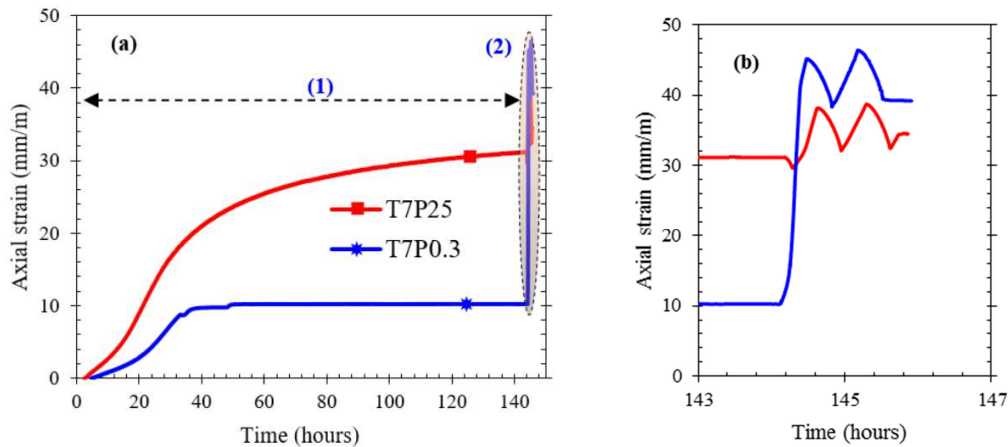
201 The oedometric cell (presented above) is used to investigate the macroscopic shrinkage of cement  
202 paste, its dependence on temperature and pressure, and also the stress strain behaviour of the cement  
203 paste. For a typical oedometric test, after mixing, the cement slurry is directly put into the oedometric  
204 cell which is kept at the test temperature. The axial stress is then increased up to the stress **during**  
205 hydration and keeps constant during the first 144 hours of hydration. At 144 hours, a mechanical  
206 loading/unloading cycle is applied with a loading rate of 3 MPa/min. For the samples hydrated under  
207 an axial stress higher than 5 MPa (Figure 5a), the loading path consists in a decrease of the axial stress  
208 to 5 MPa followed by two cycles with an increase up to 65 MPa and a decrease to 5 MPa and finally  
209 of an increase back to the initial axial stress **during** hydration. For the sample hydrated under axial  
210 stress lower than 5 MPa (Figure 5b), the loading path consists in two cycles with an increase up to  
211 65 MPa and a decrease to the axial stress **during hydration**.



212 **Figure 5. Loading path at 144 hours of hydration for different stress **during** hydration: (a) more than**  
213 **5 MPa (b) less than or equal to 5 MPa. Duration of the cycles around 1h30min, loading rate 3 MPa/min.**

214

215 The results of two typical tests in terms of axial strain as a function of time are shown in Figure 6 for  
216 two cement samples hydrated at 7°C, under 0.3 and 25 MPa, respectively. The experimental response  
217 is composed of two main parts. The first part up to 144 h for which the axial stress is kept constant  
218 (Figure 6a) shows that the macroscopic shrinkage is higher for the sample hydrated under a higher  
219 axial stress. The second part (Figure 6b) presents the response of the samples to the mechanical  
220 loading/unloading cycles and shows the lower compressibility of the sample hydrated under a higher  
221 stress. These results will be analysed in detail in the following.

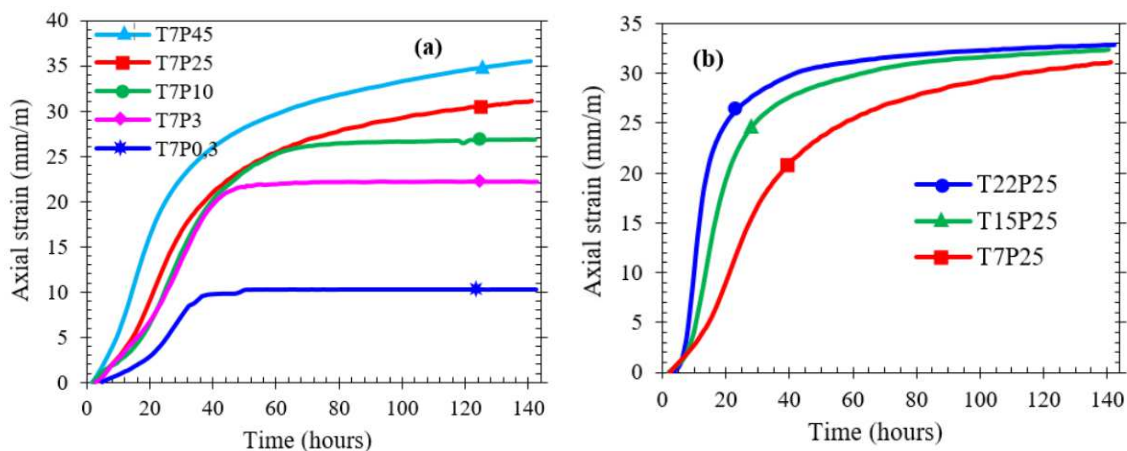


222 **Figure 6. Typical result for oedometric tests: two samples hydrated at 7°C and under 0.3 and 25 MPa**  
 223

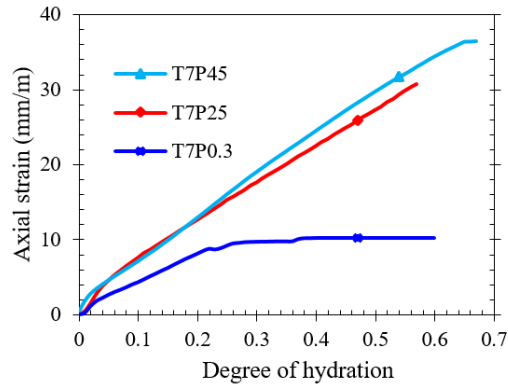
224 **4.3. Macroscopic shrinkage**

225 The macroscopic shrinkage of the cement paste is measured for different conditions of hydration in  
 226 terms of temperature and stress. At fixed temperature (7°C) **during hydration**, the cement samples are  
 227 hydrated under different axial stresses, from 0.3 MPa to 45 MPa. The evolution of axial strain as a  
 228 function of time for five samples is presented in Figure 7a, showing a progressive increase of the  
 229 macroscopic shrinkage during hydration. The deformation of the sample hydrated under 0.3 MPa  
 230 becomes stable after 40 hours of hydration. This happens a little later, at about 50 and 60 hours  
 231 hydration, respectively for the sample hydrated under 3 MPa (T7P3) and 10 MPa (T7P10). The  
 232 deformation of the samples hydrated under 25 MPa (T7P25) and 45 MPa (T7P45) continues to  
 233 increase at 144 hours. These results show that at a given time, the macroscopic shrinkage is  
 234 significantly higher for hydration under higher stress. However, one should note that this observation  
 235 is influenced to some extent by the pressure dependency of cement hydration kinetics, as presented in  
 236 Figure 4. The results of three experiments under various pressures, for which calorimeter results were  
 237 available, are plotted in Figure 8 as a function the degree of hydration. Two distinguished responses  
 238 can be observed for macroscopic shrinkage under high and low pressures: the samples hydrated under  
 239 high pressure, i.e. 25 and 45 MPa, show almost similar response in terms of a quasi linear macroscopic  
 240 shrinkage evolution with the degree of hydration, while the sample hydrated under a low pressure of  
 241 0.3 MPa, shows a more nonlinear response. The initial slope of the axial strain – **degree of** hydration  
 242 response at the very beginning is very close to the one of the high-pressure samples. This should  
 243 correspond to the chemical shrinkage of the cement hydration, as before percolation and formation of  
 244 a solid skeleton all chemical shrinkage is transformed to the macroscopic shrinkage. A value of 0.044  
 245 – 0.060 can be found for the chemical shrinkage of this cement which is very close to the values  
 246 presented in the literature [32, 5, 33, 34, 18, 35].

247 The measured axial strain, i.e. the macroscopic shrinkage, at 144 hours of hydration increases with the  
 248 axial stress during hydration (Figure 9a). Reddy et al. (2009) also observed this increase of  
 249 macroscopic shrinkage with the increase of stress applied on the cement paste during its hydration.  
 250 Figure 7b presents the evolution of the axial strain of the cement paste as a function of time, for  
 251 hydration under constant axial stress (25 MPa) but at different temperatures (7, 15 and 22°C). As  
 252 observed in this figure, the effect of temperature is more pronounced during the first 60 hours of  
 253 hydration and seems to vanish with the advancement of the reaction. The long-term effects of  
 254 temperature and pressure on macroscopic shrinkage at 144h are presented in Figure 9 for 7°C  
 255 temperature (variable stress) and 25 MPa axial stress (variable temperature). It can be seen that the  
 256 effect of temperature is less significant compared to that of stress (Figure 9b). This is of course partly  
 257 due to the relatively narrow range of the studied temperatures. The results show that higher pressure  
 258 during hydration leads to higher compaction of the samples. The density of the hydrated material is  
 259 thus expected to be higher for samples hydrated under higher pressure. The observed macroscopic  
 260 shrinkage during hydration results from strongly coupled phenomena: at the very early age and before  
 261 the percolation the slurry is under an isotropic stress state with the pore pressure equal to the total  
 262 pressure, i.e. zero Terzaghi effective stress. The water consumption during hydration results in a  
 263 progressive pore pressure decrease in the samples and thus to an increase of the effective stress.  
 264 Moreover, the progressive hardening of the material results in development of shear stress in the  
 265 sample which is in oedometric condition. These stress changes result in mechanical deformation of the  
 266 material which can be a combination of deformations with elastic, elastoplastic and viscous nature. For  
 267 the samples under lowest pressures, 0.3 MPa and 3 MPa, the water consumption may result in a partial  
 268 desaturation of the material. A better understanding of the mechanisms of deformation of the samples  
 269 needs a coupled chemo-poro-mechanical simulation of the presented experiments, taking into account  
 270 the above-mentioned phenomena.



271 **Figure 7. Experimental measures of macroscopic shrinkage of cement paste during the first 144 hours of**  
 272 **hydration: (a) constant temperature during hydration (7°C) [T7P10 and T7P3 are from [15]], (b) constant**  
 273 **axial stress during hydration (25 MPa).**



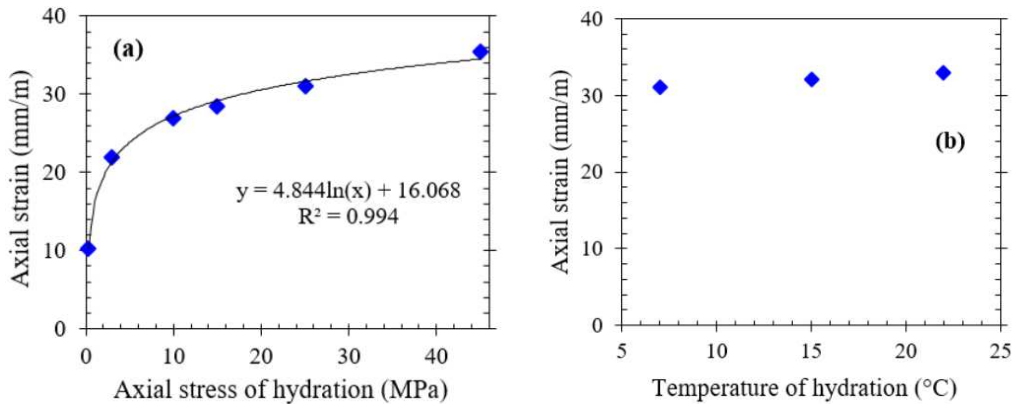
275

276

**Figure 8. Macroscopic shrinkage of three samples of cement paste hydrated at 7°C and under different stresses**

277

278



279

**Figure 9. Macroscopic shrinkage of the cement paste at 144 hours of hydration: (a) effect of the axial stress, (b) effect of temperature of hydration.**

280

281

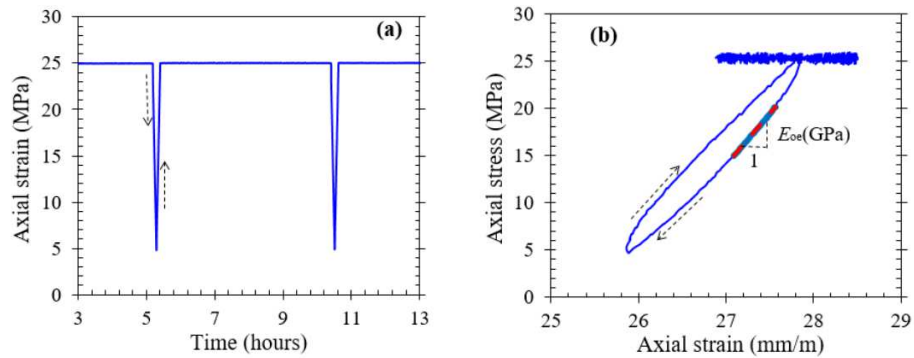
**4.4. Oedometric moduli**

282

The oedometric moduli are measured in the performed oedometric experiments. The static modulus is measured by performing mechanical unloading and reloading on the hydrating cement paste in undrained condition. The measurements are performed for three samples M-T7P15, M-T7P25 and M-T7P45 hydrating at the same temperature (7°C), but under different axial stresses 15, 25 and 45 MPa, respectively. “M-” before the test conditions is related to “modulus”. The loading path is similar for the three conditions. It is presented in Figure 10a for the sample M-T7P25, showing an unloading from the axial stress during hydration (i.e. 25 MPa) to 5 MPa and reloading to the stress during hydration. The unloading/reloading cycles were applied at different given times with the rate of 3 MPa/min. The duration of one unloading/reloading cycle is around 7, 13 and 27 minutes for the samples M-T7P15, M-T7P25 and M-T7P45, respectively. Considering the relatively slow hydration rate at 7°C, it can be assumed that these loading cycles are performed at constant degree of hydration. The stress-strain

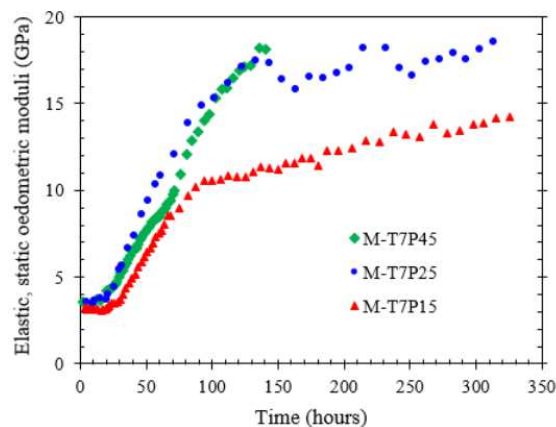
292

293 response for one cycle of sample M-T7P25 is presented in Figure 10b. It can be assumed that the cycle  
 294 is performed in the elastic domain and can be used to evaluate the elastic oedometric modulus. We  
 295 chose to evaluate the tangent oedometric modulus on the unloading slope for axial stress between 12  
 296 and 7 MPa, between 20 and 15 MPa and between 30 and 15 MPa respectively for the samples  
 297 hydrated under 15, 25 and 45 MPa. The different intervals are chosen to prevent the parasite strains  
 298 observed at the beginning of the unloading or reloading, which are due to the mechanical system of the  
 299 frame and to the inertia of the LVDT.  
 300



301 **Figure 10. Loading path and stress-strain response for a cement hydrated at 7°C and under 25 MPa**  
 302 **(sample M-T7P25)**  
 303

304 The oedometric moduli for the three samples M-T7P15, M-T7P25 and M-T7P45 are given in Figure  
 305 11 as a function of time. During the first 15 or 20 hours of hydration, the moduli are relatively  
 306 constant and vary between 3 and 4 GPa. These values, as also observed by Vu (2012), are slightly  
 307 higher than the bulk modulus of water (around 2.2 GPa). The difference is probably due to the  
 308 presence of the clinker grains in the cement slurry. The stable values within this time window shows  
 309 that the cement paste behaves like fluid with suspensions. There is a fast increase of the modulus  
 310 between 20 and 90 hours for the sample M-T7P15 and between 20 and 140 hours for the samples M-  
 311 T7P25 and M-T7P45. This fast increase is followed by a slighter increase for the later hydration ages.



312

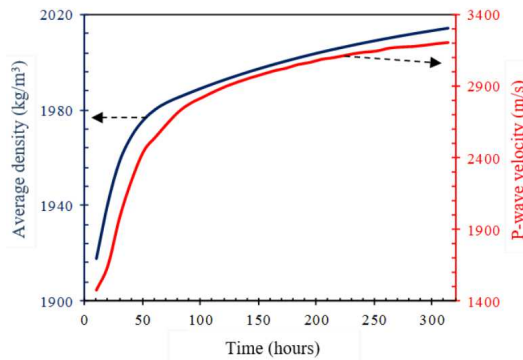
313 **Figure 11. Elastic, static oedometric modulus as a function of time for three cement samples hydrating at**  
 314 **7°C and under 15, 25 and 45 MPa.**

315

316 The Ultrasonic Cement Analyser (UCA) is used to measure the ultrasonic P-wave velocity in the  
 317 cement paste during hydration. The dynamic oedometric modulus  $E_{\text{oed}}^{\text{dyn}}$  can then be calculated using  
 318 the following relation as a function of the P-wave velocity  $V_p$ , by knowing the density of the sample  $\rho$   
 319 **Error! Reference source not found..**

320 
$$E_{\text{oed}}^{\text{dyn}} = \rho V_p^2 \quad (3)$$

321 At ultrasonic frequency, the pore pressure generated within the cement paste during the wave's  
 322 travelling do not have enough time to diffuse out of the sample. The measured dynamic modulus is  
 323 thus considered as undrained oedometric modulus. For the samples hydrated under pressure, the  
 324 average density of the cement paste increases during hydration, due to the compaction effect. For the  
 325 cement sample hydrated under 25 MPa, the evolution of the average density and of the P-wave  
 326 velocity during hydration are given in Figure 12. The density (resp. the P-wave velocity) of the cement  
 327 increases from approximately 1910 kg/m<sup>3</sup> (resp. 1400 m/s) for the slurry state to around 2000 kg/m<sup>3</sup>  
 328 (resp. 3200 m/s) after 300 hours of hydration. The dynamic modulus, calculated using equation (3) is  
 329 presented in Figure 13 and compared with the static modulus measured under similar condition of  
 330 hydration. The results exhibit a dynamic modulus slightly higher than the static modulus. This is in  
 331 agreement with existing experimental results showing that the dynamic modulus is generally higher  
 332 than the static modulus for different materials [36, 37, 38].

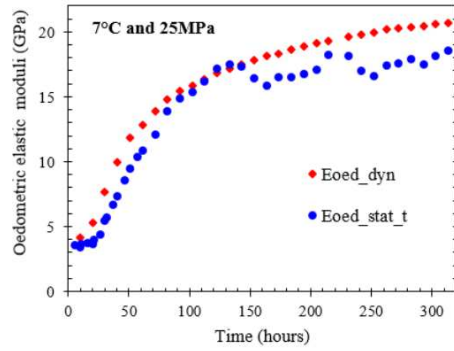


333

334 **Figure 12. Average density and ultrasonic P-wave velocity as a function of time for the cement sample**  
 335 **hydrating at 7°C and under 25 MPa [28].**

336





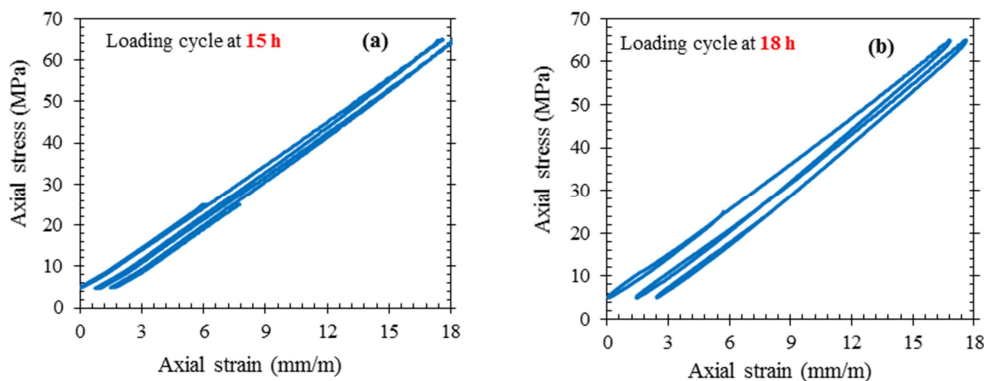
337  
338  
339  
340

**Figure 13. Comparison between the dynamic and static elastic “undrained” oedometric moduli for samples hydrated at 7°C and under 25 MPa on the UCA and the oedometric cell, respectively.**

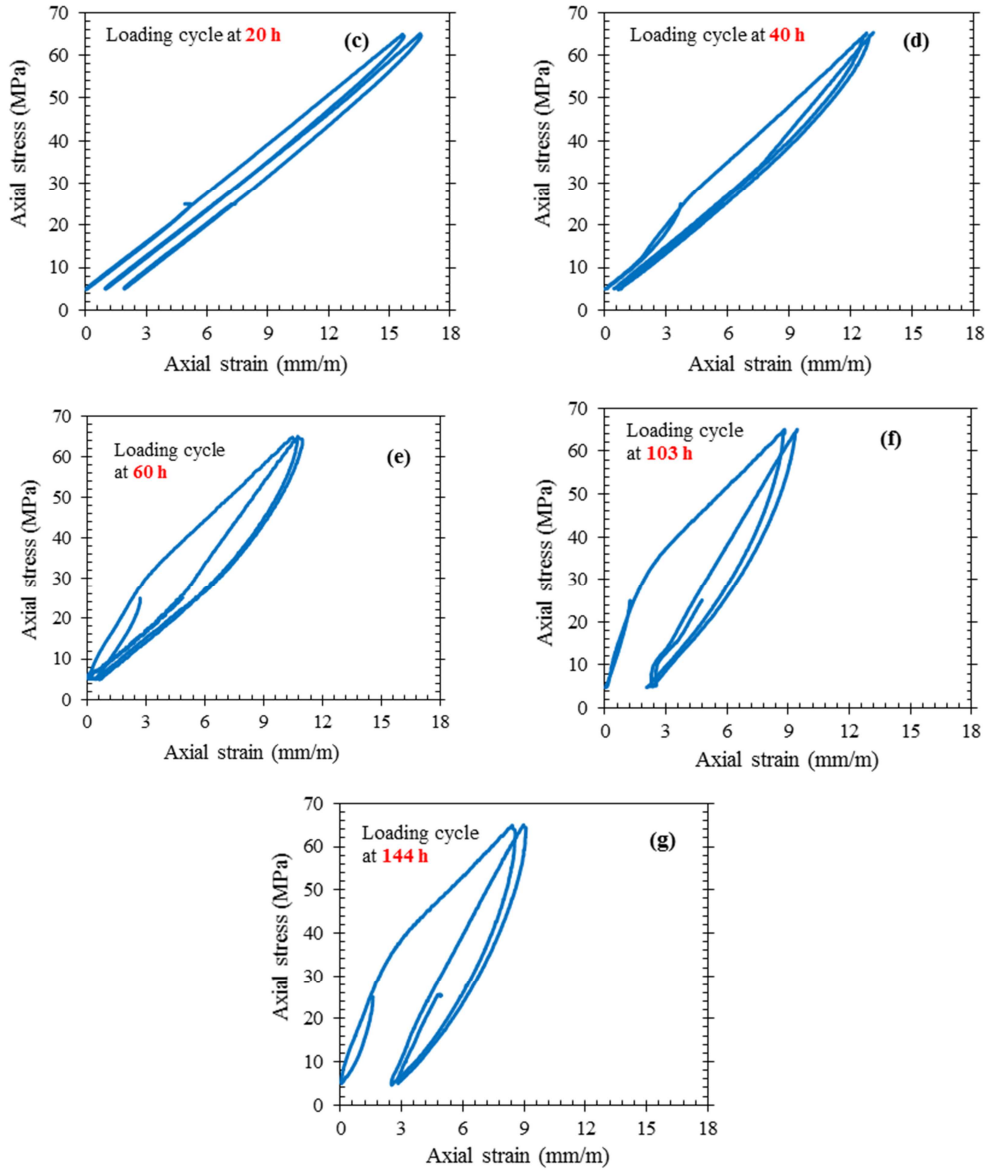
341 **4.5. Stress–strain response**

342 **4.5.1. Effect of age**

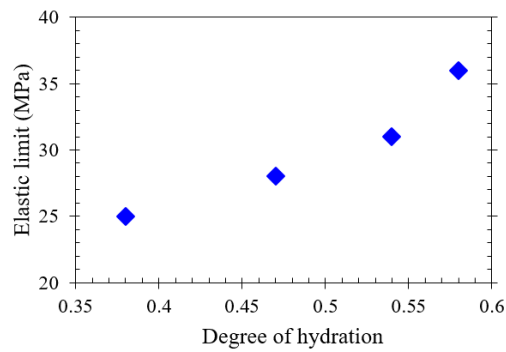
343 Seven samples of cement paste, with the same composition (Table 1 & Table 2), hydrated at 7°C and  
344 under 25 MPa, are submitted to mechanical unloading/reloading cycles as shown in Figure 5a. Each  
345 sample has been loaded at a different age, 15, 18, 20, 40, 60, 103 and 144 h. The results are presented  
346 in Figure 14. The loading cycles applied at earlier age show a quite linear stress-strain response with  
347 non-recoverable strains in unloading. The results show a progressively non-linear stress-strain  
348 response for later loadings particularly after 40h. During the first loading (5 → 65 MPa), two main  
349 slopes can be distinguished on the samples loaded after 20 hours of hydration. These slopes may  
350 characterize the elastic and elastoplastic domain of the response with a transition at the elasticity limit.  
351 As presented in Figure 15, this stress limit increases with the degree of hydration (or age) at which the  
352 mechanical loadings are applied. Moreover, the slope of the first unloading/reloading cycle  
353 (25 → 5 → 25 MPa) increases with the age of the cement paste. This is in agreement with the increase  
354 of the elastic parameters of the cement paste with hydration as is observed also in the measured  
355 oedometric modulus during hydration (Figure 11 & Figure 13).







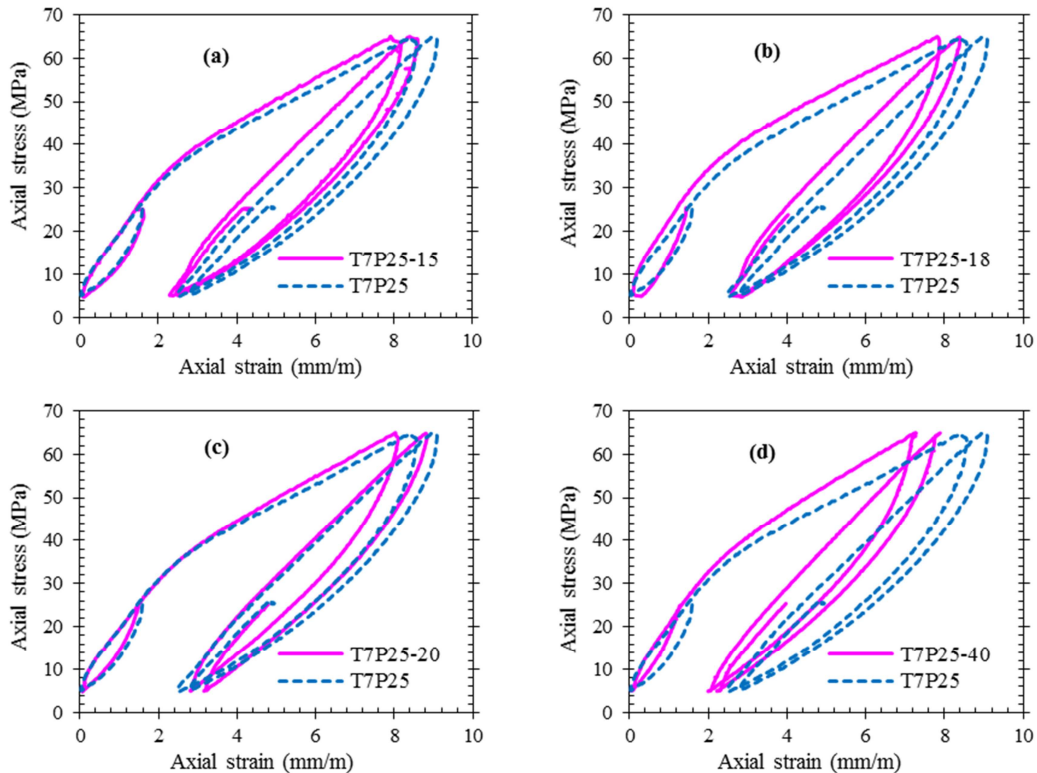
356 **Figure 14. Stress-strain behaviour at different age of cement samples hydrated under similar oedometric**  
 357 **conditions (7°C and 25 MPa)**  
 358

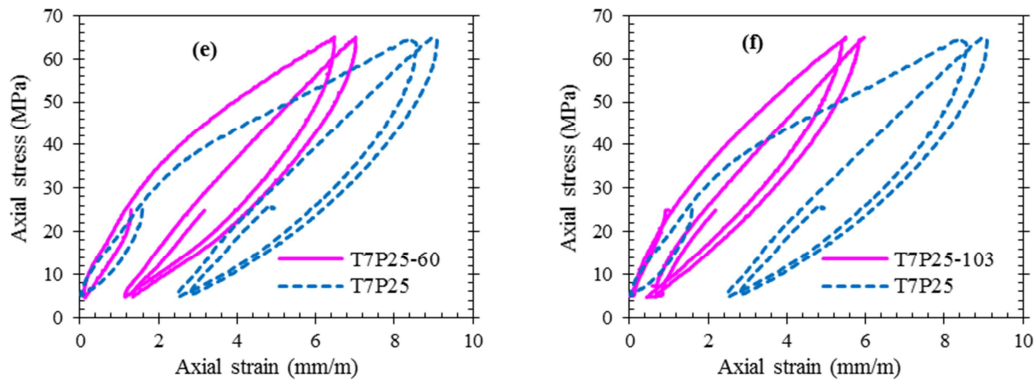


359 **Figure 15. Elastic limit as a function of the degree of hydration**  
 360

362 **4.5.2. Effect of loading history**

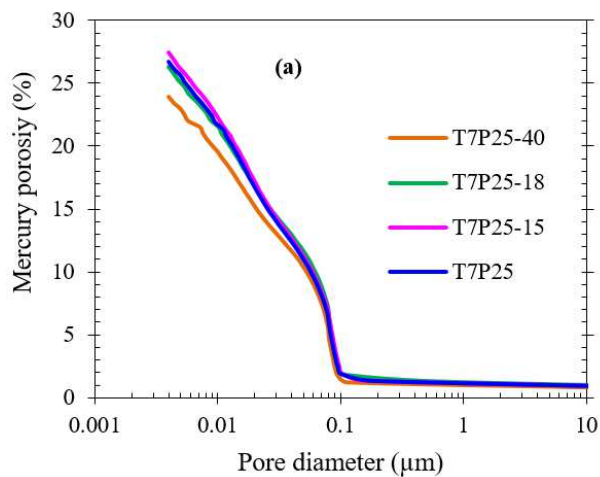
363 As explained in the introduction, various mechanical loadings can be applied to the cement sheath in  
 364 an oil-well and it is important to investigate the effect of these early-age loadings on the long-term  
 365 behaviour of the cement paste. In order to analyse the effect of the previous mechanical loading cycles  
 366 on the stress-strain behaviour of cement paste at later age of hydration, the samples presented in the  
 367 Figure 14 have been for a second time submitted to the same mechanical loading at 144 hours. The  
 368 effect of this first mechanical loading on the cement behaviour is analysed by comparing the result of  
 369 their second loading with the stress-strain response of the sample submitted for the first time at  
 370 144 hours (Figure 14g). On the following figures, the samples are identified by the hydration  
 371 conditions and the time of their first mechanical loading. For example, T7P25-40 (solid line)  
 372 represents the sample hydrated at 7°C and under 25 MPa on which the first mechanical loading is  
 373 applied at 40 h. The mechanical loading previously applied at 15, 18 and 20 h (Figure 16a, b and c)  
 374 seem to have little effect on the stress-strain behaviour at 144 hours. The stress-strain curves are quite  
 375 similar, even though we can observe that the previously loaded samples are a little less deformable.  
 376 This is much more visible and significant for the samples loaded previously after 40 hours of  
 377 hydration. The stress-strain response of these samples shows a lower deformability, higher moduli and  
 378 lower irrecoverable strains in unloading.





379 **Figure 16. Effect of previous mechanical loadings applied within 15 h and 103 h on the stress–strain**  
 380 **behaviour of the cement paste submitted to the same mechanical loadings at 144 hours.**  
 381

382 After the loading at 144 hours, the samples T7P25, T7P25-15, T7P25-18 and T7P25-40 were  
 383 immediately removed from the oedometric cell and kept into distilled and deaerated water at ambient  
 384 conditions for at least 3 months. The mercury porosity measurements are then performed and the  
 385 results are shown in Figure 17. **It is worth nothing that** the only difference between these samples is  
 386 the age at which the first mechanical loading was applied. It can be observed that the first loading  
 387 applied at 15 or 18 h has no significance effect on the mercury porosity, as compared to sample T7P25  
 388 on which no further loading cycle has been applied (Figure 17). The loading applied at 40 h reduced  
 389 significantly the mercury porosity. In Table 4, it is shown that the mercury porosity as well as the total  
 390 porosity are smaller in sample T7P25-40 as compared to the other samples. The mercury and total  
 391 porosity are in the same order as those found by Ghabezloo et al. **Error! Reference source not**  
 392 **found..** The decrease of the porosity with the application of the mechanical loading cycles is related to  
 393 the compaction of the cement sample.



394 **Figure 17. Mercury porosity on cement paste as a function of the reached pore diameter**  
 395

396  
397

**Table 4. Physical properties of four samples conserved in water at ambient conditions for at least 3 months after the application of the mechanical loading cycles at 144 hours.**

	<b>T7P25</b>	<b>T7P25-15</b>	<b>T7P25-18</b>	<b>T7P25-40</b>
Mercury porosity (%)	26.7	27.5	26.2	23.4
Saturated density (g/cm <sup>3</sup> )	2.022	2.022	2.010	2.005
Total porosity (%)	43.5	43.1	43.3	42.8

398

399

#### **4.5.3. Effect of temperature and pressure conditions during hydration**

400

- **At 144 hours of hydration**

401

The stress-strain responses of the samples hydrated under different conditions of temperature and axial

402

stress are presented in Figure 18 (the first phases of these experiments are presented in Figure 7). The

403

experiments performed at 7°C under different initial axial stresses are shown in Figure 18a.

404

Comparing the curves shows that the samples hydrated under higher stress are less deformable during

405

the first loading. For samples hydrated under relatively high stress (10 and 25 MPa), for the first

406

loading until 65 MPa the sample shows a quasi bilinear response corresponding to an elastic response

407

under lower stresses and then an elasto-plastic response for higher stresses with a smooth transition at

408

about 25 to 30 MPa axial stress. The following unloading-reloading cycles result in an almost linear

409

response with a little hysteresis which may be attributed to the viscous behaviour of the cement paste

410

[12]. The samples hydrated under relatively low stress (0.3 and 3 MPa) show a more complex

411

response under the first loading up to 65 MPa. A first change in the slope of the stress-strain curve is

412

observed at 20 to 25 MPa axial stress, similar to the one observed for samples hydrated under higher

413

stress, but a second slope change and a significant hardening of the material is observed under higher

414

axial stress of about 45 to 50 MPa. The physical mechanism behind this hardening of the material can

415

be explored considering an elasto-plastic constitutive law for hydrating cement paste based on these

416

experimental results [28]. Figure 18b presents the results of the experiments performed on cements

417

hydrated under 25 MPa axial stress at different temperatures between 7 and 22°C. The results show

418

quite similar response, which can be related to the narrow range of studied temperatures. One can see

419

however that the samples hydrated under higher temperature are less deformable. This can be related

420

to the increase of the cement hydration rate with temperature. The analysis of the results presented in

421

Figure 7 and Figure 18 shows a strong coupling between the macroscopic shrinkage and stress-strain

422

response of the cement paste. An appropriate constitutive model for the hydrating cement paste should

423

capture this coupling and the physical mechanisms behind the observed response of this material.

424

Another general observation, which can be made based on these experimental results, corresponds to

425

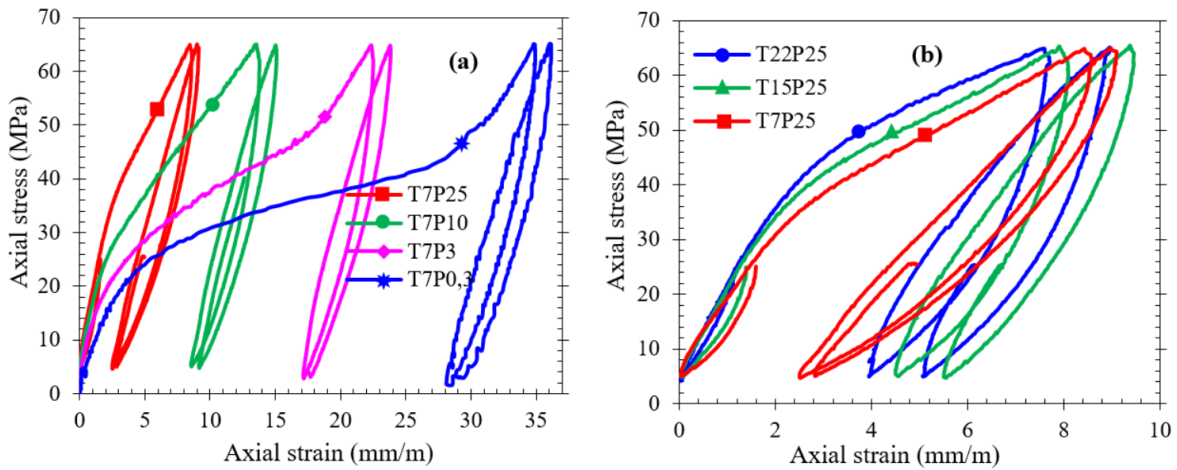
the significantly higher deformability of the cement paste hydrated under relatively low stress. This

426

higher deformability shows the higher risk of creation of a micro-annulus at shallower depths of a

427

well.

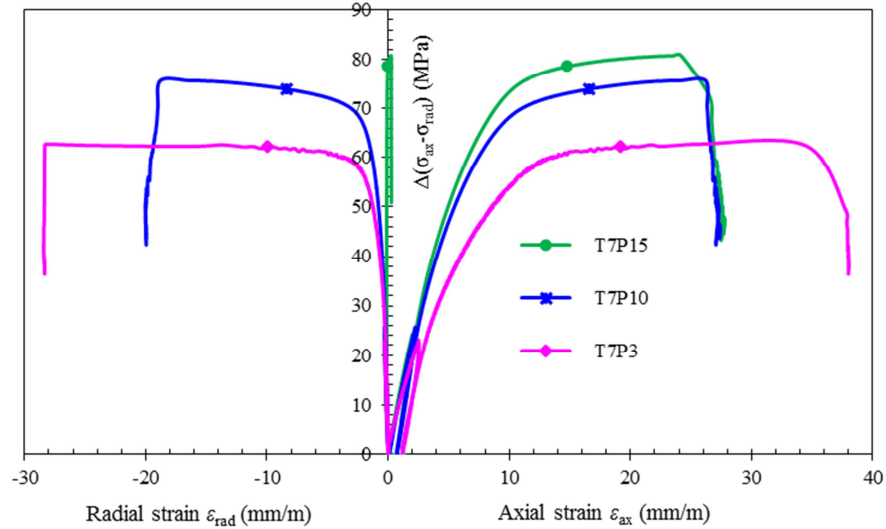


428 **Figure 18. Experimental measures of stress–strain behavior of cement paste at 144 hours of hydration: (a)**  
 429 **constant temperature during hydration (7°C), (b) constant axial pressure during hydration (25 MPa).**  
 430

431 • **After 3 months of hydration**

432 Three samples hydrated at the same temperature (7°C) but under different axial stresses 3, 10 and  
 433 15 MPa (T7P3, T7P10, T7P15) have been submitted to triaxial testing after 3 months of hydration.  
 434 The samples were submitted to the same mechanical loading path at 144 hours as presented in Figure  
 435 5. The samples were then kept at the ambient temperature in saturated condition for 3 months before  
 436 performing triaxial experiments. These experiments have been performed under a confining pressure  
 437 of 25 MPa. The differential stress as a function of axial and radial strain is presented in Figure 19. The  
 438 results clearly show that the stress-strain behaviour of the cement paste is affected by the condition of  
 439 hydration during the first 144 hours. Samples hydrated under lower stress show higher deformability  
 440 and lower shear strength. This confirms once again the higher potential of micro-annulus formation at  
 441 shallower depths.

442



443

444 **Figure 19. Results of the triaxial tests on the cement paste hydrated under oedometric conditions during**  
 445 **the first 144 hours and kept at ambient conditions for 3 months. The confining pressure was 25 MPa [15]**  
 446

447

448 The mechanical static and dynamic properties of the samples are presented in Table 5. The static  
 449 moduli have been evaluated in the unloading-reloading cycles. The static drained bulk and Young  
 450 moduli increase with the increase of the axial stress during hydration applied on the samples during  
 451 the first 144 hours of hydration. As commonly observed, the dynamic bulk modulus and Poisson's  
 452 ratio are higher compared to the static values. The explanation of this difference can be traced to the  
 453 fact that the dynamic parameters are measured under quasi-undrained conditions whereas the statics  
 454 ones are obtained under drained conditions. It can also be due to the amplitude of deformation which  
 455 is much smaller for dynamic measurements (around  $10^{-7} - 10^{-6}$  in dynamic measurements, and  $10^{-3}$  in  
 456 static measurements [39]) as also mentioned by Oku and Eto (1993). The effect of hydration  
 457 conditions in these samples shows that the cement paste stiffness in long-term increases with the  
 increase of the stress applied during the early-age of hydration.

458

459 **Table 5. Static and dynamic parameters of three samples of cement paste hydrated under oedometric**  
 460 **conditions during the first 144 hours and kept at ambient conditions for 3 months.**

Samples	Static parameters			Dynamics parameters		
	T7P15	T7P10	T7P3	T7P15	T7P10	T7P3
$K_d$ (GPa)	7.56	7.16	6.95	16.32	16.15	16.25
$G$ (GPa)	7.08	6.56	5.56	8.21	8.36	8.34
$\nu$	0.14	0.15	0.18	0.31	0.30	0.30
$E$ (GPa)	16.18	15.08	13.17			
$E_{\text{oed}}$ (GPa)	16.99	15.91	14.36			
$\Delta(\sigma_{\text{ax}} - \sigma_{\text{rad}})_{\text{max}}$ (MPa)	81	76	64			

## 461        **5. Conclusion**

462        The early-age mechanical behaviour of a class G oil-well cement paste is experimentally investigated  
463        using a specially designed cell, which permits mechanical loading application from the first hour of  
464        hydration, even before the setting of the cement. The macroscopic shrinkage of the cement paste as  
465        well as its stress-strain response under oedometric loading are studied for various pressures during  
466        hydration, from 0.3 to 45 MPa, and for temperatures during hydration from 7 to 30°C. The results  
467        showed a significant increase of the macroscopic shrinkage with the pressure during hydration. At a  
468        given age, the cement paste hydrated under lower pressures exhibits a significantly higher  
469        deformability when submitted to a mechanical loading cycle. This result shows a higher risk of  
470        creation of micro-annulus at shallower depth during the mechanical loadings, for example during a  
471        casing test. The stress-strain response of the cement paste strongly depends on the cement age. When  
472        submitted to a loading cycle at different times, a mostly linear and reversible response observed at the  
473        very early age is progressively transformed to a highly nonlinear response and increasing irreversible  
474        deformations. At a given time, the mechanical response of the cement paste submitted to a loading  
475        cycle depends on the loading history. This is an important point showing that the simulation of the  
476        cement sheath response in an oil well needs a complete modelling of its behaviour from the placement  
477        to the current state, including various applied loads. This is confirmed also for the long-term behaviour  
478        by performing classical triaxial experiments after 3 months hydration on cement samples with  
479        different loading history at early age. The samples submitted to lower stress at early age show higher  
480        deformability. In the studied ranges of pressure and temperature, the pressure has a much more  
481        significant effect on the mechanical response of the cement, compared to the temperature effect.  
482        However, one should note that a relatively narrow range of mostly low temperature are investigated  
483        here, mainly to slow down the hydration rate for performing loading cycles application in a relatively  
484        constant hydration degree. This study will be extended in the future by exploring a broader range of  
485        higher temperatures.

## 486        **6. Acknowledgments**

487        The authors gratefully acknowledged TOTAL for supporting this research. They also wish to thank  
488        Joselin DE-LA-IGLESIA, Edmond POYOL and Sandrine ANNET-WABLE from TOTAL for  
489        performing calorimeter experiments and Nicolas CRUZ from ACEI for his assistance in the testing  
490        program.

## 491        **7. References**

492

- [1] L. A. Behrmann, J. L. Li, A. Venkitaraman and H. Li, "Borehole Dynamics During Underbalanced Perforating," *Society of Petroleum Engineers*, no. SPE 38139, pp. 17-24, 1997.
- [2] M. J. Thiercelin, B. Dargaud, J. F. Baret and W. J. Rodriguez, "Cement Design Based on Cement Mechanical Response," *Society of Petroleum Engineers*, no. SPE 38598, pp. 337-348, 1997.
- [3] P. A. Parcevaux and P. H. Sault, "Cement Shrinkage and Elasticity: A New Approach for a Good," *SPE Annual Technical Conference and Exhibition*, pp. 1-7, 1984.
- [4] H. Justnes, D. Van Loo, B. Reyniers, J. Skalle, P. Sveen and E. J. Sellevold, "Chemical shrinkage of oil well cement slurries," *Advances in Cement Research*, vol. 7, pp. 85-90, 1995.
- [5] S. K. Lyomov, K. R. Backe, P. Skalle, O. B. Lile, H. Justnes and J. Sveen, "Shrinkage of Oil Well Cement Slurries," *The Petroleum Society*, pp. 1-7, 1997.
- [6] S. Ghabezloo, J. Sulem and J. Saint-Marc, "The effect of undrained heating on a fluid-saturated hardened cement paste," *Cement and Concrete Research*, vol. 39, pp. 54-64, 2009.
- [7] S. Ghabezloo, "Association of macroscopic laboratory testing and micromechanics modelling for the evaluation of the poroelastic parameters of a hardened cement paste," *Cement and Concrete Research*, vol. 40, p. 1197-1210, 2010.
- [8] M.-H. Vu, J. Sulem and J.-B. Laudet, "Effect of the curing temperature on the creep of hardened cement paste," *Cement and Concrete Research*, vol. 42, pp. 1233-1241, 2012.
- [9] S. Ghabezloo, "Micromechanics analysis of thermal expansion and thermal pressurization of a hardened cement paste," *Cement and Concrete Research*, vol. 41, no. 5, pp. 520-532, 2011.
- [10] S. Ghabezloo, J. Sulem, S. Guedon, F. Martineau and J. Saint-Marc, "Poromechanical behaviour of hardened cement paste under isotropic loading," *Cement and Concrete Research*, vol. 38, no. 12, pp. 1424-1437, 2008.
- [11] S. Ghabezloo, "Effect of the variations of clinker composition on the poroelastic properties of hardened class G cement paste," *Cement and Concrete Research*, vol. 41, pp. 920-922, 2011.
- [12] M.-H. Vu, J. Sulem, S. Ghabezloo, J.-B. Laudet, A. Garnier and S. Guédon, "Time-dependent behaviour of hardened cement paste under isotropic loading," *Cement and Concrete Research*, 2012.



- [13] S. Bahafid, S. Ghabezloo, M. Duc, P. Faure and J. Sulem, "Effect of the hydration temperature on the microstructure of Class G cement: C-S-H composition and density," *Cement and Concrete Research*, vol. 95, pp. 270-281, 2017.
- [14] S. Bahafid, S. Ghabezloo, P. Faure, M. Duc and J. Sulem, "Effect of the hydration temperature on the pore structure of cement paste: Experimental investigation and micromechanical modelling," *Cement and Concrete Research*, vol. 111, pp. 1-14, 2018.
- [15] N. Agofack, S. Ghabezloo and J. Sulem, "Effect of loading history on mechanical properties of hardened oilwell cement," 2018, 52nd U.S. Rock Mechanics/Geomechanics Symposium, 17-20 June, Seattle, Washington, ARMA-2018-953.
- [16] API-10B-2, Recommended Practice for Testing Well Cementing, 24th Edition ed., American Petroleum Institute, 2012, pp. 1-52.
- [17] C. Baumgarte, M. Thiercelin, & K. D. SPE and S. Dowell, "Case Studies of Expanding Cement To Prevent Microannular Formation," *Society of Petroleum Engineers*, no. SPE 56535, pp. 1-8, 1999.
- [18] B. R. Reddy, Y. Xu, D. Gray, Halliburton, P. D. Pattillo and B. America, "Cement-Shrinkage Measurement in Oilwell Cementing--A Comparative Study of Laboratory Methods and Procedures," *Society of Petroleum Engineers*, no. SPE 103610, pp. 104-114, 2009.
- [19] D. P. Bentz and O. M. Jensen, "Mitigation strategies for autogeneous shrinkage cracking," *Cement and Concrete Composites*, vol. 26, pp. 677-685, 2004.
- [20] API, "Shrinkage and Expansion in Oilwell Cements," API Publishing Services, Washington, 1997.
- [21] B. R. Reddy, A. Santra, D. McMechan, D. Gray, C. Brenneis and R. Dunn, "Cement Mechanical-Property Measurements Under Wellbore Conditions," *Society of Petroleum Engineers*, pp. 33-38, 2007.
- [22] M. Abuhaikal, S. Musso, J. Thomas and F.-J. Ulm, "An apparatus for Dissecting Volumetric Changes in Hydrating Cement Paste," *Mechanics and Physics of Creep, Shrinkage and Durability of Concrete*, pp. 316-323, 2013.
- [23] N. C. Ludwig and S. A. Pense, "Conduction calorimeter for measuring heat of hydration of Portland cement at elevated temperature and pressure," *ACI Journal, Proc.*, vol. 53, 1956.

- [24] H. Taylor, *Cement Chemistry*, London: Academic Press, 1990.
- [25] J. J. Thomas, "A new approach to modeling the nucleation and growth kinetics of tricalciumsilicate hydration," *J. Am. Ceram. Soc.*, vol. 90, no. 10, p. 3282–3288, 2007.
- [26] B. Bresson, F. Meducin and H. Zanni, "Hydration of tricalcium silicate (C3S) at high temperature and high pressure.," *Journal of Material Science*, vol. 37, pp. 5355-5365, 2002.
- [27] M. H. Vu, Effet des contraintes et de la température sur l'intégrité des ciments des puits pétroliers, PhD thesis, Ecole des Ponts ParisTech, 2012, p. 240.
- [28] N. Agofack, "Comportement des ciments pétroliers au jeune âge et integrite des puits," PhD thesis, Université Paris Est, Paris, 2015.
- [29] A. K. Schindler, "Effect of Temperature on Hydration of Cementitious Materials," *ACI Materials Journal*, vol. 101, no. 1, pp. 72-81, 2004.
- [30] E. Gallucci, X. Zhang and K. Scrivener, "Influence de la température sur le développement microstructural des bétons," in *Septième édition des Journées Scientifiques du Regroupement francophone pour la recherche et la formation sur le béton*, Toulouse, France, 2006.
- [31] E. Gallucci, X. Zhang and K. L. Scrivener, "Effect of temperature on the microstructure of calcium silicate hydrate (C-S-H)," *Cement and Concrete Research*, vol. 53, pp. 185-195, 2013.
- [32] E.-i. Tazawa, S. Miyazawa and T. Kasai, "Chemical shrinkage and autogenous shrinkage of hydrating cement paste," *Cement and Concrete Research*, vol. 25, no. 2, pp. 288-292, 1995.
- [33] P. Mounanga, A. Khelidj, A. Loukili and V. Baroghel-Bouny, "Predicting Ca(OH)<sub>2</sub> content and chemical shrinkage of hydrating cement pastes using analytical approach," *Cement and Concrete Research*, vol. 34, pp. 255-265, 2004.
- [34] M. Bouasker, P. Mounanga, P. Turcry, A. Loukili and A. Khelidj, "Chemical shrinkage of cement pastes and mortars at very early age: Effect of limestone filler and granular inclusions," *Cement & Concrete Composites*, vol. 30, pp. 13-22, 2008.
- [35] W. Yodsudjai and K. Wang, "Chemical shrinkage behavior of pastes made with different types of cements," *Construction and Building Materials*, vol. 40, pp. 854-862, 2013.

- [36] J.-K. Kim and S.-H. Han, "Effect of temperature and age on the relationship between dynamic and static elastic modulus of concrete," *Cement and Concrete Research*, vol. 34, pp. 1219-1227, 2004.
- [37] T. Oku and M. Eto, "Relation between static and dynamic Young's modulus of nuclear graphites and carbon," *Nuclear Engineering and Design*, vol. 143, pp. 239-243, 1993.
- [38] J. Sabbagh, J. Vreven and G. Leloup, "Dynamic and static moduli of elasticity of resin-based materials," *Dental materials*, vol. 18, pp. 64-71, 2002.
- [39] G. Mavko, T. Mukerji and J. Dvorkin, *The Rock Physics Handbook : Tools for seismic Analysis of Porous Media*, Second edition ed., Cambridge: Cambridge University Press, 2009.

493

494